Management and Production Engineering Review
Volume 15 • Number 2 • June 2024 • pp. 42–56
DOI: 10.24425/mper.2024.151129

Multi-weld Quality Optimization of Friction Stir Welding for Aluminium Flange Using the Grey-based Taguchi Method

Ibrahim SABRY[1], Mohamed ELWAKIL[2], A.M. HEWIDY[1]

[1] *Department of Mechanical Engineering, Benha Faculty of Engineering, Benha University, Benha, 13511, Egypt*
[2] *Department of Production Engineering and Mechanical Design, Faculty of Engineering, Tanta University, Tanta, Egypt*

Received: 12 September 2023
Accepted: 06 April 2024

Abstract
Friction stir welding (FSW) is gaining traction as a preferred technique due to its potential to reduce heat input and enhance the mechanical properties of welded joints. However, the path to commercializing FSW for flange joints is not without challenges. Two primary obstacles are the complexity of the welding path and the intricate design requirements for the fixtures. These factors contribute to the difficulty in determining the ideal weld settings and process parameters, which are critical for achieving optimal results. The current study addresses these challenges by applying FSW to flange joints using custom-engineered fixtures. These fixtures are meticulously designed to hold the pipes and plates securely during the welding process. The focus of the research is on optimizing the multi-performance characteristics of FSW for Al 6063 flange joints through the hybrid Grey-based Taguchi method. The integrity of the weld joint is assessed by examining various mechanical properties within the weld zone, including rotation speed, travel speed, tool profile, and shoulder diameter. The study identifies the optimal parameter settings for the FSW process: a rotation speed of 3000 rpm, a travel speed of 3 mm/min2, a shoulder diameter of 20 mm, and a conical tool profile. Under these ideal conditions, the welded material exhibited a tensile strength of 170.169 MPa, a hardness of 63.7709 HV, and a corrosion rate of 0.022 mm/year. These findings underscore the effectiveness of the optimized FSW process in producing robust and durable flange joints.

Keywords
Flange, Friction stir welding, L9 Taguchi, GRA, hybrid GRA-Taguchi.

Introduction

The objective of material progress is to discover novel metallic constituents capable of satisfying the increasing need for enhanced strength and reduced weight. Aluminum alloys are widely regarded as the optimal selection, especially in situations where extensive production is necessary. Aluminum alloys provide a notable combination of high specific strength and exceptional resistance to corrosion, rendering them the favored material for vital structural elements in industries such as aircraft, pipeline, automobile, transportation, military, shipbuilding, civil engineering, and others. Structures that are essential and exposed to different levels of stress during operation may undergo material fatigue. Hence, it is imperative to take into account the fatigue strength while designing structural components (Sabry et al., 2022a). Welding is a widely used and efficient technique for connecting metal structures. Conventional fusion or resistance welding faces challenges when dealing with aluminum alloys because of their elevated heat and electrical conductivity. Several aluminum alloys (Weman, 2003). The Welding Institute (TWI) in Cambridge has devised a method to address the difficulty of joining materials that were previously deemed difficult to weld or were thought unweldable. Friction stir welding (FSW) was developed during the 1990s. The process entails harnessing friction and agitating the welded substance to merge it into a solid form. Friction stir welding (FSW) is highly advantageous for joining aluminum alloys, and it is also applicable to a wide range of other materials (Argesi et al., 2021).

***Corresponding author**: Ibrahim Sabry – Department of Mechanical Engineering, Benha Faculty of Engineering, Benha University, Benha, 13511, Egypt, phone: (+2) 01003719980, e-mail: ibrahim.sabry@bhit.bu.edu.eg*

© 2024 The Author(s). This is an open access article under the CC BY license (http://creativecommons.org/licenses/by/4.0/)

Literature review

The most popular welding method for threaded flange connections is TIG (inert tungsten gas) welding because of its superior results. A professional welder who can create strong connections between the components being joined without leaving any weak places in the joint area is needed for this type of welding (Sabry & Zaafarani, 2017). Fusion welding techniques like TIG and metal inert gas (MIG) produce higher temperatures than solid-state underwater friction stir welding (Sabry & Zaafarani, 2017). Fusion arc welding processes use an arc temperature above the melting point of the base metal. Only the FSW technique, however, requires a temperature more significant than that of recrystallization. FSW, a modern solid-state welding process, avoids heating the base material to the point of melting by using a non-consumable tool.

Unlike all fusion welding techniques, the FSW is a stochastic process. FSW includes several welding process elements. The features of the finished product, such as the weld quality and mechanical or metallurgical properties, are therefore unclear. Numerous investigations on welding parameters have been conducted independently of welding techniques. In the majority of investigations, the plunge depth, (N), (S), and standard FSW parameters were discussed in the research publications (Sabry et al., 2022b). The welding process also heavily depends on other parameters, including dwell time, vibrational frequency, tool, and pin form. The results of some of the research studies are listed below. Pawar and Sheet identified vital factors impacting the mechanical properties and microstructure while researching to enhance the FSW of aluminum 6063 pipes (Sabry et al., 2022b). They discovered improved FSW performance results from more excellent tool (N) and lower (S) values. The pin shapes impact the joint qualities, affecting the interface's friction.

Instead of cylinder-shaped and tapered pins, spherical pins created the highest temperature at the workpieces (Ismail et al., 2015). Compared to butt FSW weld joints, more articles are available in the pipes field (Chen et al., 2015). VHN, yield power, UTS, and El% are essential for various weld connections.

Some statistical approaches and machine learning algorithms have proven helpful for data analysis and output prediction from experimental data. Research on ANN and RSA by (Thekkuden & Mourad (2019) for process optimization and porosity prediction. Lakshminarayanan and Balasubramanian showed that ANN was more accurate than response surface analysis when predicting the tensile strength of FSW AA 7039 joints (Lakshminarayanan & Balasubramanian, 2009). Similar outcomes were obtained by Krishnan & Subramaniam (2018), who reported that the optimal welding parameters in welds of the A.A. 6063-A319 alloy could be predicted by ANN more accurately than by the response surface method. Hu et al. used pigeon-inspired optimization combining ANN to evaluate the mechanical characteristics of several AlMg welds produced using ultrasonic-assisted FSW (Hu et al., 2020).

On the FSW of A.A. 6082-T6, Wakchaure et al. (2018) used hybrid GRA-ANN to find that (N) and (D) are the essential parameters, followed by tilt angle and tool geometry. Sabry & Moura (2021a) evaluation of the ANN-GRA simulated annealing technique to maximize UTS and VHN in F.S. welds shows that the hybrid approach is practical for modeling and optimization. According to Dewan et al. (M.W. Dewan, 2015), the adaptive ANFIS predicted the UTS of FSW more accurately than the ANN. The resilience of ANN over statistical methodologies was compared to that of Shehabeldeen et al. in their study (Taher et al., 2019). It has been proven that the ANFIS is superior to the response surface method for optimizing AA2024-AA5083 friction stir welds. According to Thekkuden & Mourad (2019), Harris–Hawks optimization, in conjunction with ANFIS, successfully determines the appropriate FSW process parameters. The optimization of process factors for achieving utmost weld strength using FSW on cryogenically aluminum 2219 alloy has been investigated by Kamal Babu et al. (2018). Integrating an ANN with the G.A. enhanced the weld's strength. In their study, Khalkhali et al. (2017) utilized the Taguchi design of experiments technique to identify the optimal combination of process criteria for lap joint FSW of AA1100 aluminum alloy. The experimental design employed in this study utilized Taguchi's L16 orthogonal array to conduct the experiments for FSW. Additionally, ANOVA was employed to evaluate the significance of the design parameters with the output parameters.

The input process parameters discussed in this study encompassed the tool's rotating speed, tilt angle, traverse speed, and pin form. The design with the highest potential was achieved by considering many output elements, such as the diameters of the grain in the weld zone, the mechanical strengths (UTS and VHN), the maximum working temperature, and the forces exerted on the tool in both the horizontal and vertical directions throughout the entire process. The mechanical qualities (Prasad & Namala, 2018) and corrosion resistance (Lee et al., 2016) of aluminum alloy joints produced by FSW are affected by factors like tool rotating speed, welding speed, and tool tilt angle. In their comprehensive analysis, Xiaocong He et al. (2014)

conducted a thorough examination of scholarly articles about numerical investigations in the field of friction stir welding, specifically focusing on works published from the year 2000 onwards. A comprehensive review was conducted on the recent advancements in numerical analysis of FSW procedures, microstructures, and the attributes of the welded joints. The discussion also encompassed important numerical considerations, including the meshing method, modeling of materials flow, and establishing failure criteria.

In their study, Meraihi et al. (2021) comprehensively analyzed the Dragonfly algorithm and its various alternatives. These alternatives were categorized into two groups: better versions and hybrid versions. In addition to the review, this paper also discusses the various uses of the Dragonfly algorithm in several domains, including image processing, machine learning, neural networks, robotics, and other technical applications. In their work, Chnoor, & Rahman (2019) provided an overview of the Dragonfly algorithm and its several iterations. Furthermore, the various forms of hybridization employed by the algorithm were also discussed.

Furthermore, the method underwent verification using the CEC-C06 2019 standard benchmark functions. The results demonstrated that the algorithm exhibited a high degree of exploration and achieved convergence faster than other algorithms, such as PSO and G.A., as reported in the existing literature. The optimal multi-objective evaluation of process parameters (namely tool speed, feed rate, and depth of cut) has been investigated by Arun Vikram Kothapalli et al. (2017) through the utilization of the Taguchi-based Dragonfly algorithm. The study examined the output qualities, including hardness, surface roughness, and tool vibration amplitude, during tangential and orthogonal turn-mill operations on a CNC vertical milling center. The obtained results were juxtaposed with the outcomes of GRA, a widely recognized technique for multi-response optimization.

In their study, Sharma et al. (2019) conducted an optimization of the FSW process parameters, including rotating speed, pin offset, diameter of shoulder, and speed of welding. This optimization aimed to enhance the quality of joints in dissimilar aluminum and copper materials. The authors employed the Taguchi-based Technique for the TOPSIS technique, for this purpose. The study examined the impact of different combinations of these factors on the joints' mechanical properties, specifically the UTS and VHN. The mechanical properties, specifically the tensile and impact strengths, of AISI 409 M ferritic stainless-steel joints with a thickness of 4 mm, produced via FSW, were investigated by Lakshminarayanan & Balasubramanian (2013) studies were conducted using a central composite rotatable design with three components and five levels. The process parameters, notably rotating speed, welding speed, and shoulder diameter, were optimized using multi-response optimization techniques involving numerical and graphical methods. The Taguchi technique was implemented to optimize the process parameters, namely rotating speed, transverse speed, and axial force, in the FSW of an Al–Mg alloy (Vijayan et al., 2010).

According to the experimental findings, it was observed that the highest UTS of 301 MPa was attained under the following conditions: a speed of rotational 650 rpm, a speed of transverse 115 mm/min, and an axial force of 17 kN. The magnitude of the strength is subject to notable impact from the speed of rotational, which constitutes a substantial proportion of 88.64% in terms of its overall contribution, alongside many other parameters. Teimouri and Baseri (2015) examined the efficacy of the fuzzy artificial bee colony imperialist competitive algorithms in predicting the FSW parameters for both forward and backward scenarios.

Most studies have only focused on enhancing FSW process parameters for plates and pipes. Additionally, unlike flanges, articles about the FSW of plates are plentiful. Concerning UTS, VHN, and C.R., As far as the authors are aware, flange joints have not been used in the FSW process. This study presents a novel methodology in Friction Stir Welding (FSW) to join flange joints. The process parameters are optimized for the FSW process parameters for flange joint welding of aluminum 6063-T3 to enhance welding efficiency, while a newly invented fixture is used for Friction Stir Welding (FSW) on a vertical milling machine.

Materials & Methods

Materials

The pipes and plates utilized in the work are made of 6063-T3 aluminium alloy and have an outside diameter of 53 mm, a wall thickness of 4 mm, and a plate thickness of 9 mm. The chemical makeup and mechanical characteristics of Tables 1 and 2 exhibit base metal. Figure 1 shows the elemental compositions of the energy dispersive spectrometry curve and the substructure of the base metal under investigation. Steel K100 is used to make the FSW tool. The details of the tool shape employed for this study are shown in Figure 2. The axial force and the pin length tilt angle were set to 4.8 mm, 10 K.N., and 32 MPa. The FSW process is depicted schematically in Figure 3. The process parameters, including the (N), (S), and (D), were set to be 3000, 2500, and 2000 rpm, as well

as 3,5 and 10 mm/min, 10,20, and 30 mm, respectively, the tensile test was conducted following ASTM D638. An analogue universal measuring machine tester with a 100 kN load was employed for the tensile test, and the VHN test based on ASTM E18-22 was carried out.

Table 1
Al 6063-T3's Composition and Properties

Wt. %	Al	Si	Fe	Cu	Mn	Mg	Cr	Zn	Ti
	96	0.6	0.35	0.1	0.1	0.9	0.1	0.1	0.1
Ultimate tensile strength				Hardness			Elongation		
195				90			10%		

Table 2
The levels of process parameters in FSW

Process Parameters	Unit	Symbol	Levels		
			–1	0	1
Rotation speed	RPM	N	3000	2000	1800
Travel speed	mm/ min	S	3	10	16
Shoulder diameter	mm	F	10	20	30
Tool profile		T	Cylindrical	Taper	Conical

Corrosion rate

Benha University's Laboratory of Metallurgy Mechanical Engineering conducts corrosion testing utilizing a link to the NOVA software, a three-electrode cell potentiostat. following ASTM G102 standards. Figure 4 depicts the corrosion test specimen's measurements. In this corrosion test, a chemical solution with a 3.5% NaCl content following the ASTM D1141 standard replaces seawater.

Hardness evaluation

The Universal Hardness Tester was used to determine Vickers's hardness. Testing for hardness is done following Figure 6.

Tensile test

Three tensile specimens have been produced for each experiment following the ASTM E8M-04 standard.

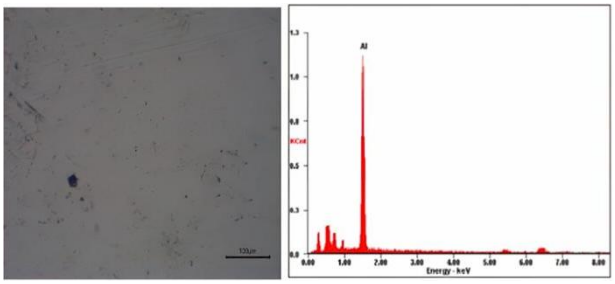

Fig. 1. (a) Base metal microstructure and (b) A.A. 6063-T3's EDS

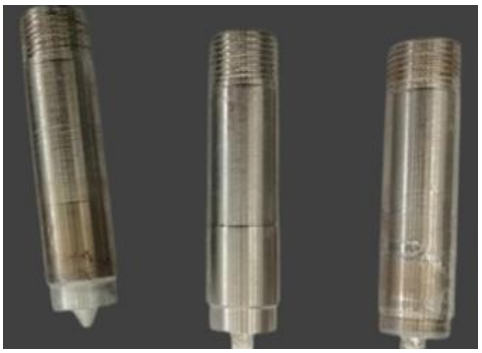

Fig. 2. The tool's geometric specifications

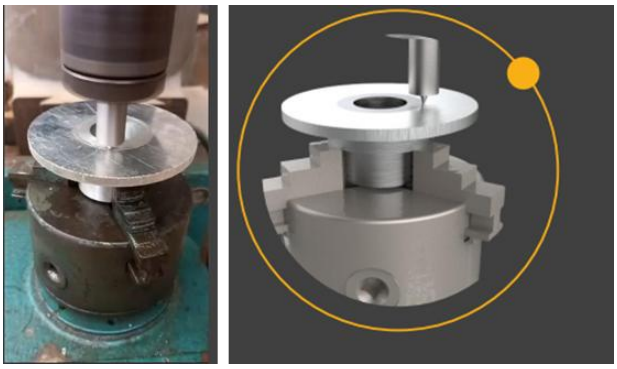

Fig. 3. Shows the fixture and set used to induce FSW for a flange in schematic form

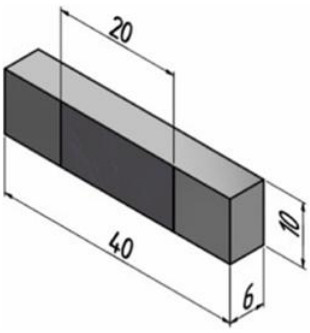

Fig. 4. Dimensions of the corrosion test

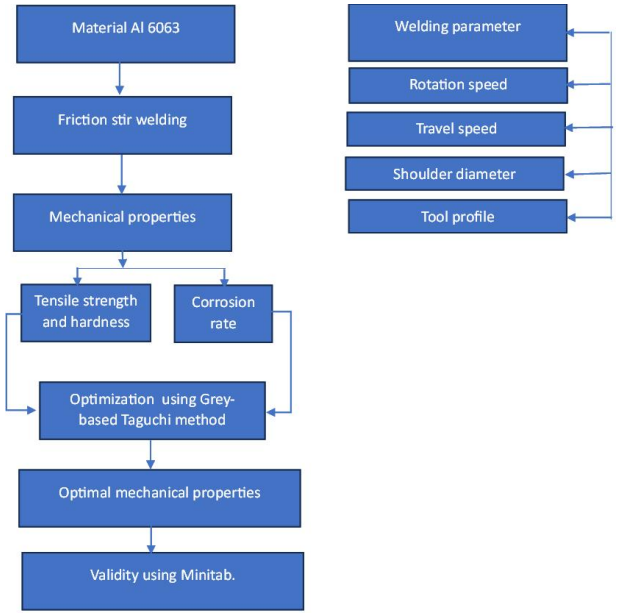

Fig. 5. Methodology

The UTS of the FSW joints was tested using universal testing equipment, and Table 3 and Figure 7 display the average of the three results.

A welding apparatus was employed, consisting of a cylindrical, tapered, and conical structure with a threaded probe featuring a cylindrical cross-section. The pin profile exhibits an initial diameter of 5 mm and a concluding diameter of 4.9 mm, demonstrating a taper rate of 1 mm per unit length of the pin.

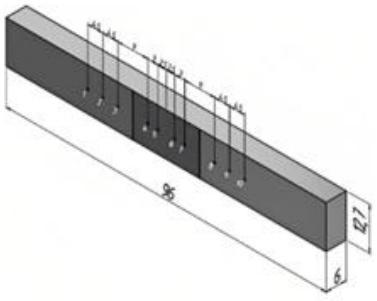

Fig. 6. Vickers hardness testing dimensions.

The welding apparatus utilized in the experiment is illustrated in Figure 2. Table 2 illustrates that the three variables of the factorial design were chosen successively throughout the three phases. The response surface methodology used 27 trials under coded conditions, utilizing a central composite design matrix.

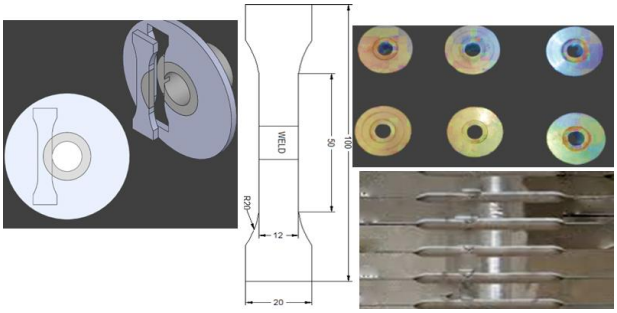

Fig. 7. The tensile test specimen, all measurements in mm

Table 3
The design matrix, experimental results, and anticipated tensile strength, hardness, and corrosion rate values

Run	FSW process parameters				Tensile strength code	Hardness code	Corrosion rate
	N	D	S	T	UTS	VHN	CR
1	3000	3	10	Cylindrical	170.00	63.54	0.2850
2	3000	10	20	Taper	167.00	60.09	0.6230
3	3000	16	30	Conical	166.39	59.30	0.3570
4	2000	3	20	Conical	162.00	57.90	0.6425
5	2000	10	30	Cylindrical	159.00	50.90	0.9365
6	2000	16	10	Taper	155.00	44.00	0.6645
7	1000	3	30	Taper	149.00	48.50	1.3290
8	1000	10	10	Conical	151.32	51.20	2.6720
9	1000	16	20	Cylindrical	148.00	47.30	2.3070

Table 3 shows the design matrix, experimental results, and anticipated tensile strength, hardness, and corrosion rate values.

Methodology

Taguchi technique

Taguchi is a Japanese quality manager, statistician, and engineer (Huang et al., 2019). Since its creation, it has optimized many procedures across a wide range of academic disciplines by optimizing the ratio of the process characteristics that can be controlled—the signal—to those that cannot be controlled—the noise—the signal-to-noise ratio is achieved. According to the required output response, three standards (SNR) are commonly used, as illustrated in equations (1), (2), and (3) (Prasanthi Kumari et al., 2018). Using this strategy, also known as the Taguchi standard orthogonal array, the best setup of the input process parameters is obtained with minimal experiments. As a minimum number of experiments are carried out to attain the ideal configuration that would produce the best-desired output instead of testing out all potential combinations of the input process parameters as is the case in the classical experiment design, time and money are saved (Benakis et al., 2020). The Taguchi technique uses the notation La(Xn) to indicate the number of experiments that must be performed. Where n is the total number of input process parameters, X is the total number of levels of input process parameters, (Ingle et al., 2023) is the total number of experiment runs.

(a) The signal-to-noise ratio for "nominal is best".

$$\eta = 10 \log \frac{1}{n} \sum_{i=1}^{n} \frac{\mu^2}{\sigma^2} \tag{1}$$

(b) Signal-to-noise ratio for "smaller the better".

$$\eta = -10 \log \frac{1}{n} \sum_{i=1}^{n} y_i^2 \tag{2}$$

(c) Signal-to-noise ratio for "larger the better".

$$\eta = -10 \log \frac{1}{n} \sum_{i=1}^{n} \frac{1}{y_i^2} \tag{3}$$

η denotes the signal-to-noise ratio (SNR), the number of experiments (η), the mean SNR, the standard deviation (σ), and the output response (y_i). The notation denotes all of them. The parameter combination that exhibits the best signal-to-noise ratio is the optimal choice. The Taguchi optimization process consists of several steps. First, the process performance or characteristics that need to be maximized, minimized, or maintained are identified. Next, the factors that control the performance are determined. Then, an appropriate orthogonal array is selected. Figure 5 presents the methodology of experimental trials conducted to obtain output responses. The output response values are analyzed to identify the optimal setting. Finally, the optimal setting is confirmed. The present study examines the three levels of N, S, D, and T with the UTS, C.R., and VHN of a similar butt joint. These performance parameters are among numerous that are being investigated. The L9 orthogonal array was subjected to Taguchi analysis using Minitab 17 software. The orthogonal array is depicted in Table 4.

Table 4
An orthogonal L9 Taguchi array

Run No	Design matrix			Estimated Mechanical parameters		
	N	S	D	UTS	VHN	CR
1	3000	3	10	Cylindrical	170.00	63.54
2	3000	10	20	Taper	167.00	60.09
3	3000	16	30	Conical	166.39	59.30
4	2000	3	20	Conical	162.00	57.90
5	2000	10	30	Cylindrical	159.00	50.90
6	2000	16	10	Taper	155.00	44.00
7	1000	3	30	Taper	149.00	48.50
8	1000	10	10	Conical	151.32	51.20
9	1000	16	20	Cylindrical	148.00	47.30

Grey-relational analysis

Instances in which the performance of a process is solely governed by a single objective or a specific set of qualities are infrequent in real-life scenarios. Regrettably, the conventional Taguchi technique is solely beneficial for a single performance characteristic. It has prompted scholars to explore several alternatives to meet this demand. The launch of GRA has garnered significant attention due to its capacity to optimize many performance metrics. Grey-relational analysis can integrate many performance characteristics of a process into a single GRG despite each performance feature having its ideal setting (Sabry et al., 2022b;

Sabry et al., 2022b; Sabry & Moura, 2021a). The technique utilizes the mechanism called grey-relational generation. The GRA method consists of multiple sequential steps. Initially, it is necessary to determine the process performance or attributes that require either maximization, minimization, or maintenance.

Furthermore, it is imperative to identify the factors that control performance. Subsequently, it is necessary to choose a suitable orthogonal array. Subsequently, experimental trials are necessary to acquire the output response values. The output response values should be normalized according to the signal-to-noise ratio requirement. Afterwards, the sequence of deviations is calculated, and ultimately, the threshold is calculated.

The suggested hybrid approach

This research proposes a hybrid method that combines the Taguchi method and GRA. This strategy is known depending on the Taguchi method. The following actions were taken (Gul et al., 2020; Krishnan et al., 2018). I was following the computation of the output response values' S/N ratios, as seen in Figure 8.

The flow chart depicted in Figure 8 incorporates the application of Taguchi analysis at step 5, wherein the objective is to determine the optimal configuration based on the major impact plots of the GRG with the input process parameters. The GRG is utilized as the output response in this research.

Results

Experimentation outcomes

The efficacy of the proposed methodology and the validity of the GRA, depending on the Taguchi method, have been established through both experimental work and optimization approaches. The simulation modelling is executed within the Minitab 18 software working platform. The FSW process was conducted using various combos of welding settings. Subsequently, the specimens were fabricated following the prescribed ASTM specifications. The organization and utilization of process factors were deemed significant in contributing to the development of the advancement model. The study outcomes are shown in Table 4. Figure 9 provides an elucidation of the microscopic image across different locations. The increase in welding speed leads to a corresponding increase in UTS, reaching its maxi-

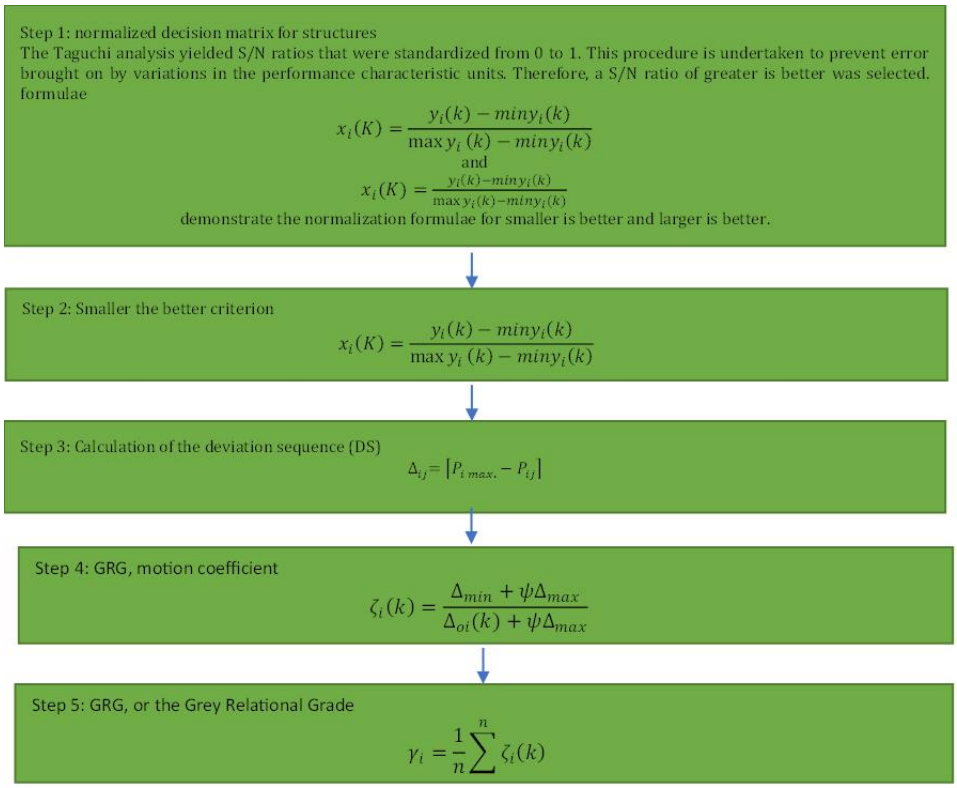

Fig. 8. Demonstrates how to use the Grey-based Taguchi process step-by-step

mum value. Figures 9 depict the exploratory findings of the study under consideration.

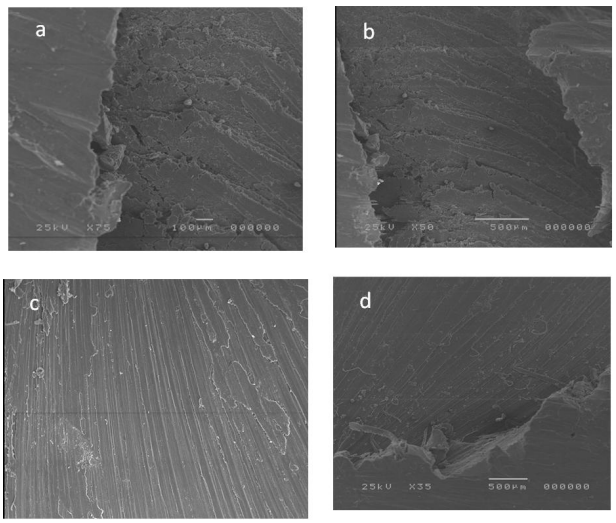

Fig. 9. Displays the microstructures observed in various locations, namely (a) TMAZ in R.S., (b) TMAZ in AS, (c) S.Z., and (d) HAZ

Flange joint UTS

One of the responses for the F.S. welded flange that was measured three times at room temperature was UTS. In Figure 10, the relationship between rotational speed and UTS is depicted. At N = 3000 rpm, D = 20 mm, and S = 3 mm/min, a conical pin profile tool produced a UTS of 283 MPa, and its joint efficiency was at or near 90%. The lowest UTS, 217 MPa, was also seen at 1000 rpm, 30 mm D, 16 mm S, and tool taper profile. Because of this, the result demonstrates that VHN and UTS are directly proportional to N and inversely proportional to S of the tool: lower S and greater N provide enough heat to join the flange B.M., consistent with previous research (Trueba et al., 2018; Sabry et al., 2023a; Hu et al., 2022).

Flange joint VHN

Three times at the nugget zone, the joint's VHN was measured. At the pick point of the curve in Figure 11, with the parameter settings of N of 3000 rpm, S of 3 mm/min, D of 20 mm, and conical tool pin profile, the higher VHN value of 63.54 VHN was attained. Accordingly, with N of 1000 rpm, S of 16 mm/min, D of 10 mm, and tapered tool pin profile, the minimum VHN value of 54.23 VHNR was noted. The highest VHN is imparted by a maximum N in conjunction with a conical tool pin.

Flange joint C.R.

At the nugget zone, the joint's C.R. was tested three times. At the pick point of the curve in Figure 12, with the parameter settings of N of 1000 rpm, S of 10 mm/min, D of 10 mm, and tapered tool pin profile, the higher C.R. value of 2.672 mm was attained. Accordingly, with N of 3000 rpm, S of 3 mm/min, D of 30 mm, and a conical tool pin profile, the minimal C.R. value of 0.285 mm was noted. The lowest C.R. is imparted when a conical tool pin is combined with the highest N, consistent with previous research (Krishnan et al., 2018).

The experimental data's signal-to-noise ratios are shown in Table 5 using the more prominent is, the better criterion. The principal impact graphs for each output response are shown in Figure 13. The optimal settings for UTS are N, S, D, and T at Level 3 (N3 S1D2 T3). That requires an N of 3000 rpm, S of 3 mm/min, D of 20 mm, and T conical. The optimal welding parameters for VHN are N of 3000 rpm, S of 3 mm/min, D of 20 mm, and T conical (N3 S1D2 T3).

In contrast, the optimal welding parameters for a corrosion rate are (N1 S2 D3 T2), N of 1000 rpm, S of

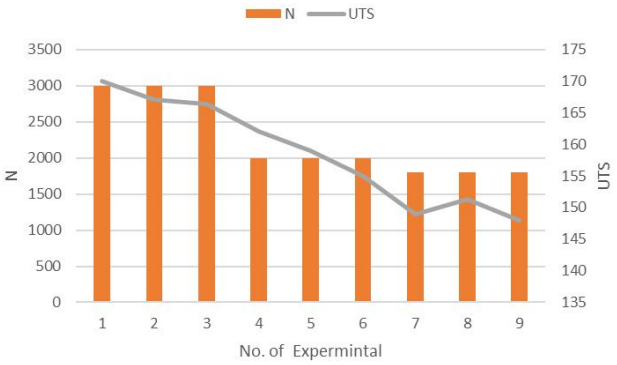

Fig. 10. Shows the impact of rotating speed on the flange material's UTS

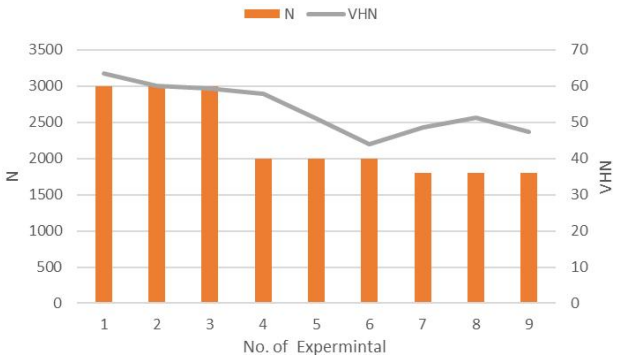

Fig. 11. Shows the impact of rotating speed on the flange material's VHN

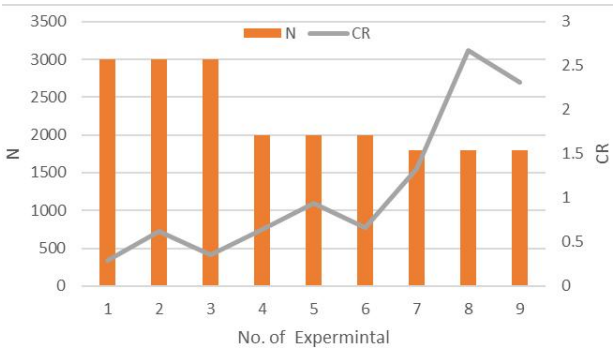

Fig. 12. Shows the impact of rotating speed on the flange material's C.R

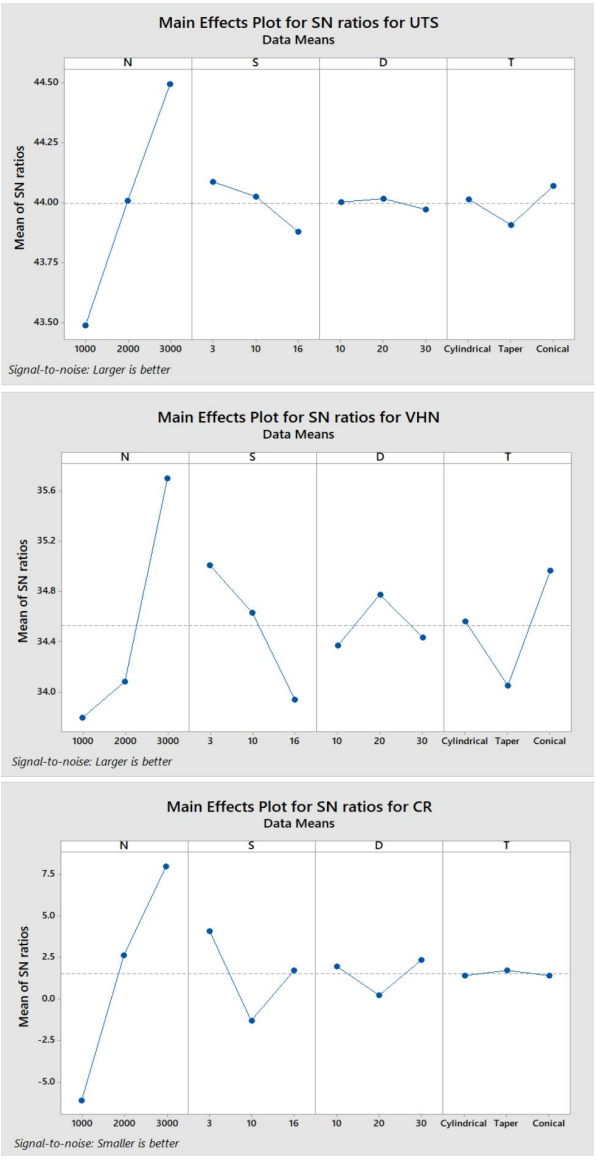

Fig. 13. Shows the output responses' main effect charts

10 mm/min, D of 30 mm, and T conical. Additionally, the output responses that are both increasing and reducing are impacted by the input process parameters, except for the UTS, which grew as the voltage increased, as shown in Figure 10.

Table 5 presents the welding parameters and the signal-to-noise ratios obtained from the experiments.

Table 5
The welding parameters and the signal-to-noise ratios obtained from the experiments

Run No	N	S	D	T	UTS	VHN	CR
1	3000	3	10	Cylindrical	48.609	40.0609	–9.361
2	3000	10	20	Taper	48.4543	40.576	–5.5367
3	3000	16	30	Conical	48.4225	40.4611	–2.4705
4	2000	3	20	Conical	48.1903	40.2536	3.5501
5	2000	10	30	Cylindrical	48.0279	40.1344	0.5698
6	2000	16	10	Taper	48.8066	40.8691	3.8425
7	1000	3	30	Taper	48.4637	40.7148	8.9466
8	1000	10	10	Conical	48.5979	40.1854	4.1102
9	3000	3	10	Cylindrical	483.4052	40.4972	10.9031

Discussion

Findings from the hybrid GRA- Taguchi method

Tables 6, 7, 8, and 9 contain the normalized signal-to-noise ratios, deviation sequences, grey-relational coefficients, and grey-relational grades and rankings, respectively. The maximum grey-relational grade achieved in experiment run 9 was 0.816936, as seen in Table 9. At this point, the N, S, D, and T values are 3000 rpm, 3 mm/min, 20 mm, and conical tool, respectively. The core effect plot for the input process parameters is depicted in Figure 14, illustrating the grey-relational grade. The optimal configuration for the various performance parameters of the FSW flange joint (UTS, VHN, and C.R.) is (N3 S1D2 T3). At level 3 (3000 rpm), the equivalent is N. At level 1 (3mm/min), the equivalent is S. At level 2 (20 mm), the equivalent is D. At level 3 (conical tool), the equivalent is T.

Using the FSW procedure, Figs. (10, 11, and 12) show the impact of welding speed on the tensile strength, hardness, and corrosion rate of 6063 aluminium alloy weld flange- joints. After reaching a max-

Table 6
The normalized S/N ratios of the output responses

Run No	N	S	D	T	UTS	VHN	CR
1	3000	3	10	Cylindrical	0.0013347	0	1
2	3000	10	20	Taper	0.00097938	0.63734224	0.81127709
3	3000	16	30	Conical	0.00090634	0.49517446	0.65996516
4	2000	3	20	Conical	0.00037301	0.23843108	0.36285845
5	2000	10	30	Cylindrical	0	0.09094284	0.50993136
6	2000	16	10	Taper	0.00178856	1	0.348429
7	1000	3	30	Taper	0.00100097	0.80908191	0.09655006
8	1000	10	10	Conical	0.00130921	0.15404603	0.33521844
9	1000	16	20	Cylindrical	1	0.53984162	0

Table 7
The normalized S/N ratios of the output response deviation sequences

Run No	N	S	D	T	UTS	VHN	CR
1	3000	3	10	Cylindrical	0.998665	1	0
2	3000	10	20	Taper	0.999021	0.362658	0.188723
3	3000	16	30	Conical	0.999094	0.504826	0.340035
4	2000	3	20	Conical	0.999627	0.761569	0.637142
5	2000	10	30	Cylindrical	1	0.909057	0.490069
6	2000	16	10	Taper	0.998211	0	0.651571
7	1000	3	30	Taper	0.998999	0.190918	0.90345
8	1000	10	10	Conical	0.998691	0.845954	0.664782
9	1000	16	20	Cylindrical	0.998665	1	0

Table 8
Displays the GRC for the normalized S/N ratios of the output responses

Run No	N	S	D	T	UTS	VHN	CR
1	3000	3	10	Cylindrical	0.33363	0.333333	1
2	3000	10	20	Taper	0.333551	0.579604	0.725981
3	3000	16	30	Conical	0.333535	0.497599	0.595213
4	2000	3	20	Conical	0.333416	0.396332	0.439699
5	2000	10	30	Cylindrical	0.333333	0.354847	0.505015
6	2000	16	10	Taper	0.333731	1	0.434189
7	1000	3	30	Taper	0.333556	0.723675	0.356265
8	1000	10	10	Conical	0.333625	0.371484	0.429265
9	1000	16	20	Cylindrical	1	0.520747	0.333333

Table 9
Displays the rankings of the output replies and the GRG

Run No	N	S	D	T	GRC	RANK
1	3000	3	10	Cylindrical	0.641575	1
2	3000	10	20	Taper	0.582515	2
3	3000	16	30	Conical	0.499546	5
4	2000	3	20	Conical	0.399821	8
5	2000	10	30	Cylindrical	0.4186	7
6	2000	16	10	Taper	0.563122	3
7	1000	3	30	Taper	0.451178	6
8	1000	10	10	Conical	0.38823	9
9	1000	16	20	Cylindrical	0.560236	4

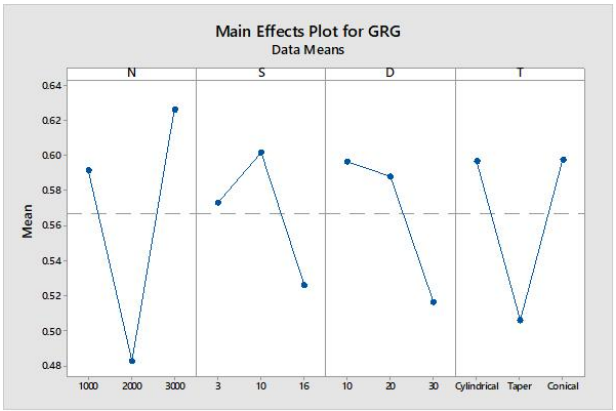

Fig. 14. The primary effect plot for the GRG for the input process parameters is depicted

imum rotation speed of 3000 rpm, travel speed of 3 mm/min, shoulder diameter of 20 mm, and conical tool profile, the tensile strength gradually diminishes, irrespective of the tool's rotational speed value, travel speed, shoulder diameter, and conical tool profile.

The mechanical qualities of the junction significantly deteriorate when the welding speed exceeds 3 mm/min since the amount of heat dissipated in the working components is less significant. Hardness and tensile strength deteriorate as a result. However, the heat input becomes less effective, and the temperature required to bring the material to the pasty condition is insufficient at welding speeds close to 10 or 16 mm/min. The causes of flaws (the tunnel effect) at the weld flange joints. To create welding flange joints of the highest quality, welding speeds closer to 3 mm/min are preferred. The mechanical qualities of the joint significantly deteriorated when the heat dissipated quantity in the parts of the works is less significant for cylindrical and taper tool profiles, which are less than conical tools. The joint mechanical qualities deteriorate significantly when the shoulder diameter values are 10 and 30 mm because the parts of the work have increased heat dissipation quantities. Tensile strength and hardness deteriorate as a result.

Using ANOVA with a 95% confidence level, the most significant variable for the multi-performance properties was identified, as shown in Table 10. All process parameters were significant, as shown by the ANOVA findings, and their p-values were less than 0.05% (Chinmay et al., 2015). The p-value test indicated that N, which contributed 79.71% and had a p-value of 0.001, was the most significant process parameter. S, D, and T came in second and third, with p-values of 0.06 and 0.07, respectively.

It is feasible to assess the usefulness of each parameter by employing variance analysis, as demonstrated by Sabry & Moura (2021b). The primary objective of ANOVA analysis is to ascertain the most influential parameter on the tensile strength of friction stir welded Al 6063 flange joints. The ANOVA analysis results for GRGs and the key ratios are presented in Table 10. The F value in Table 10 indicates the impact of each parameter on the GRG (Global Response Grade) of the flange joint. The greater the value of F, the more pronounced the oscillations of that parameter will be, resulting in a more significant impact on the quality of flange-joint qualities. The GRG of flange joints is influenced by rotational speed, travel speed, shoulder diameter, and tool profile, as indicated by the values of F. The distribution coefficient (P) is the proportion of the overall changes seen in trials that can be attributed to the effect of each parameter on the find-

Table 10
The GRG's ANOVA outcomes

Source	DF	Seq SS	Adj S.S.	Contribution	Adj MS	F-Value	P-Value
N	2	0.014333	0.014333	79.71%	0.004778	0.42	0.0744
S	2	0.001787	0.001787	20.29%	0.001787	0.16	0.0630
D	2	0.002961	0.002961	4.19%	0.002961	0.26	0.0399
T	1	0.009585	0.009585	2.53%	0.009585	0.85	0.0707
Error	1	0.056294	0.056294				
Total	8	0.070626		100.00%			

ings of GRA. The factor (P) represents the ability of each parameter to decrease the variation. By precisely managing each parameter based on the obtained value of P for that parameter, it is possible to decrease the overall variance of the process. The table displays the Percentage of distribution coefficient (%P) values for several parameters: rotational speed (79.71%), travel speed (20.29%), shoulder diameter (4.19%), and tool profile (2.53%). According to prior research conducted by Taher et al. (2019), Prasad & Namala (2018), and Meraihi et al. (2021), the rotational speed, with a maximum value of P, is the primary factor influencing the tensile strength of the joint. Among the factors significantly impacting the outcome, rotational speed, travel speed, shoulder diameter, and tool profile stand out. The welded flange-joint recorded GRGs models and the F-values of the process parameters (N, S, D, and T) are 0.42, 0.16, 0.26, and 0.85, respectively. The P-values have a probability of less than 0.05, indicating that this statistical model is statistically significant. Tables 10 indicate that N, S, D, and T are the primary machine GRG model factors.

A validation examination

A confirmatory test was conducted utilizing the ideal configuration identified by the GRA- depending on the Taguchi approach to Verify the optimization of several performance characteristics. The welding input process parameters were adjusted to their exemplary values (NTS, VHN, and C.R. readings of 170.0165 MPa, 63.892 HV, and 0.022 mm, respectively) by N = 3000 rpm, S = 3 m/min, D = 20 mm, and T = conical. These values are higher than those attained using the parameters' initial settings, confirming the validity of the GRA- depending on Taguchi, several performance characteristics optimization used by the FSW process, as illustrated in Figure 15.

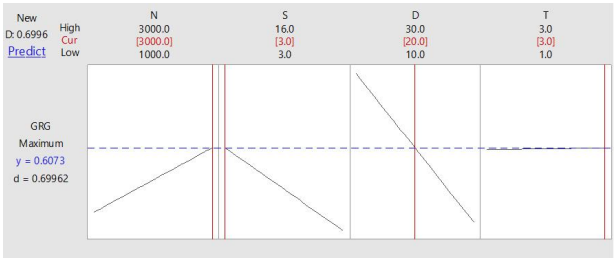

Fig. 15. Shows optimizing the factors and replies using the ANOVA response optimizer

Conclusions

Optimization modelling has proven to be an effective approach for constructing experiments. The analysis yielded the following conclusions, which aimed to optimize the FSW for flange-joint parameters for welding Al 6063 by implementing the Grey-based Taguchi method.

1. The best settings for FSW aluminium 6063 using the grey-based Taguchi multi-performance properties optimization approach are a rotation speed of 3000 rpm, travel speed of 3 mm/min, shoulder diameter of 20 mm, and tool profile conical.
2. The best results were 170.169 MPa, 63.7709 HV, and 0.022 mm for tensile strength, hardness, and corrosion rate.
3. The Vickers microhardness of the fusion zone, the tensile strength, and the corrosion rate of the weld joint have all been measured.
4. The confirmatory test to validate the optimization process showed that the Grey-based Taguchi approach is a simple yet efficient way of optimizing many performance aspects of welded joints.
5. The ANOVA and experimental methodologies yielded comparable UTS, VHN, and C.R. outcomes.

6. The proposed strategy, based on the GRA-based Taguchi technique, recommends determining the optimal parameters for FSW utilizing a Steel K100 tool operating at 3000 rpm, with a shoulder diameter of 20 mm, a conical tool profile, and a welding speed of 3 mm/min.
7. The primary obstacles to future growth in the field of FSW for flange joints are the need for significant investments in equipment and transformative measures and the readiness to adopt a radically new methodology. Applying this process outside of specialized sectors will require addressing significant technological problems in tool technology associated with high-temperature materials.

References

Anandan, B., and Manikandan, M. (2023). Machine learning approach with various regression models for predicting the ultimate tensile strength of the friction stir welded AA 2050-T8 joints by the K-Fold cross-validation method. *Materials Today Communications*, 34, 2352–4928, DOI: 10.1016/j.mtcomm.2022.105286.

Argesi, B., Shamsipur, A., and Mirsalehi, E. (2021). Preparation of bimetallic nano-composite by dissimilar friction stir welding of copper to aluminum alloy. *Transactions of Nonferrous Metals Society of China*, 31(5), 1363–1380, DOI: 10.1016/S1003-6326(21)65583-8.

Benakis, M., Costanzo, D., and Patran, A., (2020). Current mode effects on weld bead geometry and heat affected zone in pulsed wire arc additive manufacturing of Ti-6-4 and inconel 718. *Journal of Manufacturing Processes*, Elsevier Ltd, 60, 61–74, DOI: 10.1016/j.jmapro.2020.10.018.

Chen, B., Chen, K., Hao, W., Liang, Z., Yao, J., Zhang, L., and Shan, A. (2015). Friction stir welding of small-dimension Al3003 and pure Cu pipes. *Journal of Materials Processing Technology*, 233, 48–57, DOI: 10.1016/j.jmatprotec.2015.03.044.

Chinmay, S., Bhupesh, G., and Patel, V. (2015). Optimization of FSW Process Parameters for AlSiCp PRMMC Using ANOVA. *Materials Today: Proceedings*, 2(4–5), 2504–2511, DOI: 10.1016/j.matpr.2015.07.195.

Chnoor, M., and Rahman, T.A. (2019). Dragonfly algorithm and its applications in applied science survey. *Computational Intelligence and Neuroscience*, Article ID 9293617, DOI: 10.1155/2019/9293617.

Gul, M., Kalam, M.A., Mujtaba, M.A., Alam, S., Bashir, M.N., Javed, I., Aziz, U., Farid, M.R., Hassan, T., and Iqbal, S. (2020). *Multi-objective-optimization of process parameters of industrial-gas-turbine fueled with natural gas by using grey-taguchi and ANN methods for better performance*. Elsevier Ltd., 6, 2394–2402, DOI: 10.1016/j.egyr.2020.08.002.

Hu, W., Zhongwei, M., Chen, M., and Jiang, W., (2020). Improving the mechanical property of dissimilar Al/Mg hybrid friction stir welding joint by PIO-ANN. *Journal of Materials Science & Technology*, 53, 41–52, DOI: 10.1016/j.jmst.2020.01.069.

Huang, L., Hua, X., Wu, D., Jiang, Z., and Ye, Y. (2019). study on the metallurgical and mechanical properties of a GMAW-welded Al-Mg alloy with different plate thicknesses. *Journal of Manufacturing Processes*, 37, 438–445, DOI: 10.1016/j.jmapro.2018.12.017.

Ingle, A.I., Shashikala, H.D., Narayanan, M.K., Dubeto, M.T., and Gupta, S. (2023). Optimization and analysis of process parameters of melt quenching technique for multiple performances of rare earth doped barium borate glass synthesis using Taguchi's design and grey relational approach. *Results in Engineering,* 17, Article 100784, DOI: 10.1016/j.rineng.2022.100784.

Ismail, A., Awang, M., and Samsudin, H.S. (2015). *The Influence of Process Parameters on the Temperature Profile of Friction Stir Welded Aluminium Alloy 6063-T6 Pipe Butt Join.* In: Öchsner, A., Altenbach, H. (Eds.) Mechanical and Materials Engineering of Modern Structure and Component Design. Advanced Structured Materials (pp., DOI: 10.1007/978-3-319-19443-1_19), Cham: Springer.

Kamal Babu, K., Panneerselvam, K., Sathiya, P., Noorul Haq, A., Sundarrajan, S., Mastanaiah, P. and Srinivasa Murthy, C.V. (2018). Parameter optimization of friction stir welding of cryorolled AA2219 alloy using artificial neural network modeling with genetic algorithm. *The International Journal of Advanced Manufacturing Technology*, 94, 3117–3129 https://doi.org/10.1007/s00170-017-0897-6

Karuppanan, K., Panneerselvam, K., Sathiya, P., and Noorul Haq, A. (2018). Parameter optimization of friction stir welding of cryorolled AA2219 alloy using artificial neural network modeling with genetic algorithm. *The International Journal of Advanced Manufacturing Technology*, 84, 3117–3129, DOI: 10.1007/s00170-017-0897-6.

Khalkhali, A., Sarmadi, M., and Sarikhani, E. (2017). Investigation on the best process criteria for lap joint friction stir welding of AA1100 aluminum alloy via TAGUCHI technique and ANOVA. *Proceedings of the Institution of Mechanical Engineers, Part E: Journal of Process Mechanical Engineering*, 231, 329–342, DOI: 10.1177/0954408916665651.

Kothapalli, V.A., Ratnam, C.H., Lakshmi, K., and Kumar, S. (17–19 August 2017). Application of Dragonfly algorithm for optimal performance analysis of process parameters in turn-mill operations- A case study. IOP Conference Series: Materials Science and Engineering, Volume 310, *International Conference on Advances in Materials and Manufacturing Applications* (IConAMMA-2017), 310. Bengaluru, India.

Krishnan, M., and Subramaniam, S. (2018). Multiresponse optimization of friction stir corner welding of dissimilar thickness AA5086 and AA6061 aluminum alloys by Taguchi grey relational analysis. *Proceedings of the Institution of Mechanical Engineers, Part C: Journal of Mechanical Engineering Science*, 233(11), 3733-3742, DOI: 10.1177/0954406218806032.

Krishnan, M.M., Maniraj, J., Deepak, R., and Anganan, K. (2018). Prediction of optimum welding parameters for FSW of aluminium alloys AA6063 and A319 using RSM and ANN. *Materials Today Proceedings*, 5, 716–723, DOI: 10.1016/j.matpr.2017.11.138.

Kota Sankara, N., Koka Naga Sai, S., Kothapalli, A.V. (2017). Investigation on Dry Sliding Wear Behavior of Nylon66/GnP Nano-composite, Journal of The Institution of Engineers, 98(1), 71–78.

Lakshminarayanan, A.K., and Balasubramanian, V. (2009). Comparison of RSM with ANN in predicting tensile strength of friction stir welded AA7039 aluminium alloy joints. *Transactions of Nonferrous Metals Society of Chin*a, 19(1), 9–18, DOI: 10.1016/S1003-6326(08)60221-6.

Lakshminarayanan, A.K., and Balasubramanian, V. (2013). Process Parameters Optimisation for Friction Stir Welding of AISI 409M Grade Ferritic Stainless Steel. *Experimental Techniques*, 37, 59–73, DOI: 10.1111/j.1747-1567.2011.00802.x.

Lee, S.H., Lee, D.M., and Lee, K.S. (2016). Process optimisation and microstructural evolution of friction stir spot-welded Al6061 joints. *Materials Science and Technology*, 33(6), 719–730, DOI: 10.1080/02670836.2016.123066.

Meraihi, Y., Ramdane-Cherif, A., Acheli, D. and Mahseur, M. (2020). Dragonfly algorithm: a comprehensive review and applications. *Neural Computing and Application*, 32, 16625–16646. DOI: 10.1007/s00521-020-04866-y.

Mohammad, W.D., Daniel, J.H., Warren, L., Muhammad, A.W., Ayman M., (2015). Prediction of tensile strength of friction stir weld joints with adaptive neuro-fuzzy inference system (ANFIS) and neural network. *Materials & Design*, 92, 288–299, DOI: 10.1016/j.matdes.2015.12.005.

Prasad, D., and Namala, K. (2018). Process Parameters Optimization in Friction Stir Welding by ANOVA. *Materials Today:* Proceedings, 5, 4824–4831, DOI: 10.1016/j.matpr.2017.12.057.

Prasanthi Kumari, N., Hyma Laksmi, T.V., Bhavani, D., Mohana Durga, G. (2018). Weighted Transformation and Wavelet Transforms-Based Image Resolution and Contrast Enhancement. In: Singh, R., Choudhury, S., Gehlot, A. (eds.) Intelligent Communication, Control and Devices. *Advances in Intelligent Systems and Computing*, vol. 624. Springer, Singapore, DOI: 10.1007/978-981-10-5903-2_179.

Sabry, I., and Zaafarani, N.(2017). Dry and underwater friction stir welding of aa6061 pipes - a comparative study. *IOP Conference Series Materials Science and Engineering*, 1091(1)–012032, DOI: 10.1088/1757-899X/1091/1/012032. Egypt.

Sabry, I., and Moura, A.H.I. (2021a). Friction Stir Welding Process Parameters Optimization Through Hybrid Multi-Criteria Decision-Making Approach. *International Review on Modelling and Simulations*, 14(1), 32–39, DOI: 10.15866/iremos.v14i1.19537.

Sabry, I., and Moura, A.H.I. (2021b). Study on Underwater Friction Stir Welded AA 2024-T3 Pipes Using Machine Learning Algorithms. *ASME 2021 International Mechanical Engineering Congress and Expositio*, DOI: 10.1115/IMECE2021-71378. Online – ASME.

Sabry, I., Thekkuden, D.T., and Mourad, A. (2022a). TOPSIS – GRA Approach to Optimize Friction Stir Welded Aluminum 6061 Pipes Parameters. *Advances in Science and Engineering Technology International Conferences* (ASET), pp. 1–6, DOI: 10.1109/ASET53988.2022.9734821. Dubai, United Arab Emirates.

Sabry, I., Thekkuden D.T., Mourad A.-H.I., and Khan S.H. (2022b). Optimization of Tungsten Inert Gas Welding Parameters using Grey Relational Analysis for joining AA 6082 Pipes. *Advances in Science and Engineering Technology International Conferences* (ASET), pp. 1–6, DOI: 10.1109/ASET53988.2022.9735100. Dubai, United Arab Emirates.

Sabry, I., Mourad, AH.I., Alkhedhe, M., Qazani, M.R.C., and El-Araby, A. (2023a). A comparative study of multiple-criteria decision-making methods for selecting the best process parameters for friction stir welded Al 6061 alloy. *Welding International*, 37, 626–642, DOI: 10.1080/09507116.2023.2270896.

Sharma, N., Khan, Z.A., Siddiquee, A.N., and Wahid, M. (2019). Multi-response optimization of friction stir welding process parameters for dissimilar joining of Al6101 to pure copper using standard deviation based

TOPSIS method. *Proceedings of the Institution of Mechanical Engineers, Part C: Journal of Mechanical Engineering Science*, 233(18), 6473–6482, DOI: 10.1177/0954406219858628.

Taher, A. Shehabeldeen, Jianxin, Z., Xu, S., Yajun, Y., and Xiaoyuan, J. (2019). Comparison of RSM with ANFIS in predicting tensile strength of dissimilar friction stir welded AA2024–AA5083 aluminium alloys. *Procedia Manufacturing*, 37, 555–562, DOI: 10.1016/j.promfg.2019.12.088.

Teimouri, R., and Baseri, H. (2015). Forward and backward predictions of the friction stir welding parameters using fuzzy-artificial bee colony-imperialist competitive algorithm systems. *Journal of Intelligent Manufacturing*, 26, 307–319, DOI: 10.1007/s10845-013-0784-4.

Thekkuden, D.T., and Mourad, A. (2019). Investigation of feed-forward back propagation ANN using voltage signals for the early prediction of the welding defect. *SN Applied Science*, 1, DOI: 10.1007/s42452-019-1660-4.

Trueba, L., Torres, M.A., and Johannes (2018). Process optimization in the self-reacting friction stir welding of aluminum 6061-T6. *International Journal of Material Forming*, 11, 559–57, DOI: 10.1007/s12289-017-1365-4.

Vijayan, S., Raju, R., Subbaiah, K., Sridhar, N., and Rao, S.R.K. (2010). Friction stir welding of Al–Mg alloy optimization of process parameters using Taguchi method. *Experimental Techniques*, 34, 37–44, DOI: 10.1111/j.1747-1567.2009.00563.x.

Wakchaure, K.N., Thakur, A.G., and Gadakh, V. (2018). Multi-Objective Optimization of Friction Stir Welding of Aluminium Alloy 6082-T6 Using hybrid Taguchi-Grey Relation Analysis- ANN Method. *Materials Today: Proceedings*, 5(2), 7150–7159, DOI: 10.1016/j.matpr.2017.11.380.

Xiaocong, H., Fengshou, G., and Andrew, B. (2014). A review of numerical analysis of friction stir welding. Progress in Materials Science, 65, 1–66, DOI: 10.1016/j.pmatsci.2014.03.003.